



Multispectral Fusion for Synthetic Aperture Radar (SAR) Image Based Framelet Transform

Mohammed Hussein Miry

Department of Electrical and Electronic Engineering, University of Technology

email: Mohammed_miry@yahoo.Com

Received: 10/1/2011

Accepted: 9 /3/2011

Abstract-The technique of fusing a panchromatic (Pan) SAR image that has a high-spatial and low-spectral resolution with multispectral (MS) SAR images that have a low-spatial and high spectral resolution is very useful in many remote sensing applications that require both high-spatial and high-spectral resolution. In this paper, method for fusion SAR image is proposed based on framelet transform and new selection rule. The framelet transform is nearly shift-invariant with desired properties, short support, and symmetry. In the selection rule of proposed method, max rule is replaced with new relation depending on input SAR image. The proposed method is compared with other method such as HIS, PCA and wavelet methods. A quality of fused image is calculated based on the combination entropy, the correlation coefficient and the peak signal to noise ratio. It is showed from simulation result the quality measured for proposed method can indicate the information content of the fused image is higher compared to the information content of the input panchromatic and multispectral images, also its noticed the proposed method provides richer information comparing with other methods.

Keywords – Fusion, Multispectral, Panchromatic, SAR Image, Framelet Transform

1. Introduction

In many remotely sensing applications, complementary information contained, respectively, in the two categories of imagery is both useful for studying the nature of the image areas, therefore, fusion of synthetic aperture radar (SAR) image is very important to better understanding of the observed objects [1,2]. To date, many techniques and software tools for fusing SAR images have been developed. The well-known methods include the intensity–hue–saturation (IHS) color model, and principal component analysis (PCA), both IHS and PCA mergers are based on the same principle: to separate most of the spatial information of the MS image from its spectral information by means of linear transforms. The IHS transform separates the spatial information of the MS image as the intensity (I) component. In the same way, PCA separates the spatial information of the MS image into the first principal component [3]. The limitation of these methods is that some distortion occurs in the spectral characteristics of the original MS images. Recently, developments in wavelet analysis have providing a potential solution to this problem by provides a high spectral quality in fused SAR images [4]. The paper is organized as follows: Section 2, describes the theoretical basis of the framelet transform. In section 3, the IHS color conversion will be introduced and motivated. In section 4, the stages of proposed fusion method is introduced. In section 5, the factors for quantitative analysis are introduced. Simulation results of the proposed method are shown in section 6. Then, the proposed fusion is compared to HIS, PCA and wavelet methods. Finally, Section 7 gives the conclusions.

2. Framelet Transform

Framelet are very similar to wavelets but have some important differences. With frame, we can achieve better time-frequency localization than is possible with bases. Wavelet frames are shift invariant while wavelet cannot be. Besides Framelet producing symmetry, tight frame filterbanks are shorter and result in smoother scaling and wavelet functions [5].

2.1 A Symmetric Tight Wavelet Frame with Two Generators

Perfect Reconstruction Conditions and Symmetry Condition: The perfect reconstruction (PR) conditions for the three-band filterbank, which are illustrated in Figure 1, can be obtained by the following two equations [5]:

$$\sum_{i=1}^2 H_i(z)H_i(z^{-1}) = 2 \quad (1)$$

$$\sum_{i=1}^2 H_i(-z)H_i(z^{-1}) = 0 \quad (2)$$

The PR conditions can also be written in matrix form as

$$H^T(z)H(z^{-1}) = I, \quad (3)$$

Where

$$H(z) = \begin{pmatrix} H_0(z) & H_0(-z) \\ H_1(z) & H_1(-z) \\ H_2(z) & H_2(-z) \end{pmatrix}$$

Also, if $h_0(n)$ is compactly supported, then a solution $\{h_1(n), h_2(n)\}$ to Eq.(3) exists if and only if

$$|H_0(z)|^2 + |H_0(-z)|^2 < 2, \quad |z|=1. \quad (4)$$

A wavelet tight frame with only two symmetric or antisymmetric wavelets is generally impossible to obtain with a compactly supported symmetric scaling function $\phi(t)$. However, Petukhov states a condition that the lowpass filter $h_0(n)$ must satisfy so that this becomes possible [6]. Therefore, if $h_0(n)$ is symmetric, compactly supported, and satisfies Eq.(4),

then an (anti)symmetric solution $\{h_1(n), h_2(n)\}$ to Eq.(3) exists if and only if all the roots of

$$2 - H_0(z)H_0(z^{-1}) + H_0(-z)H_0(-z^{-1}) \quad (5)$$

have even multiplicity.

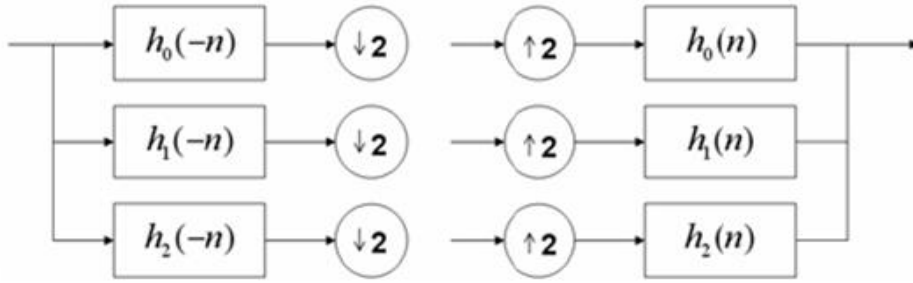


Fig 1: A three-band perfect reconstruction filterbank

Case $H_2(z) = H_1(-z)$: The goal is to design a set of three filters that satisfy the PR conditions in which the lowpass filter, $h_0(n)$, is symmetric and the filters $h_1(n)$ and $h_2(n)$ are each either symmetric or antisymmetric. There are two cases. Case I denotes the case where $h_1(n)$ is symmetric and $h_2(n)$ is antisymmetric. Case II denotes the case where $h_1(n)$ and $h_2(n)$ are both antisymmetric. The symmetry condition for $h_0(n)$ is:

$$h_0(n) = h_0(N-1-n), \quad (6)$$

where N is the length of the filter $h_0(n)$. We dealt only with Case I of even-length filters. Solutions for Case I can be obtained from solutions where $h_2(n)$ is a time-reversed version of $h_1(n)$ (and where neither filter is (anti)symmetric). To show this, suppose that $h_0(n)$, $h_1(n)$, and $h_2(n)$ satisfy the PR conditions and that

$$h_2(n) = h_1(N-1-n), \quad (7)$$

Then, by defining

$$h_1^{new} = \frac{1}{\sqrt{2}}(h_1(n) + h_2(n-2d)), \quad (8)$$

$$h_2^{new} = \frac{1}{\sqrt{2}}(h_1(n) - h_2(n-2d)), \quad d \in Z \quad (9)$$

the filters h_0 , h_1^{new} and h_2^{new} also satisfy the PR conditions, and h_1^{new} and h_2^{new} are symmetric and antisymmetric as follows:

$$h_1^{new}(n) = h_1^{new}(N_2-1-n),$$

$$h_2^{new}(n) = h_2^{new}(N_2-1-n),$$

where $N_2 = N + 2d$.

The polyphase components of the filters $h_0(n)$, $h_1(n)$, and $h_2(n)$ are given in [5] with symmetries in Eq.(6) and Eq.(7) satisfy the PR conditions. Figure 2 shows the frequencies of filters are used to construct framelet transform with FIR. The filter $h_0(n)$ will be a low-pass

(scaling) filter, while $h_1(n)$ and $h_2(n)$ will both be high-pass (wavelet) filters [7]. To use the double-density discrete wavelet transform for 2D signal processing, we must implement a two dimensional analysis and synthesis filter bank structure. This can simply be done by alternatively applying the transform first

to the rows then to the columns of an image. This gives rise to nine 2D subbands, one of which is the coarse (or low frequency) subband, and the other eight of which make up the eight detailed (or high frequency) subbands as shown in Figure 3.

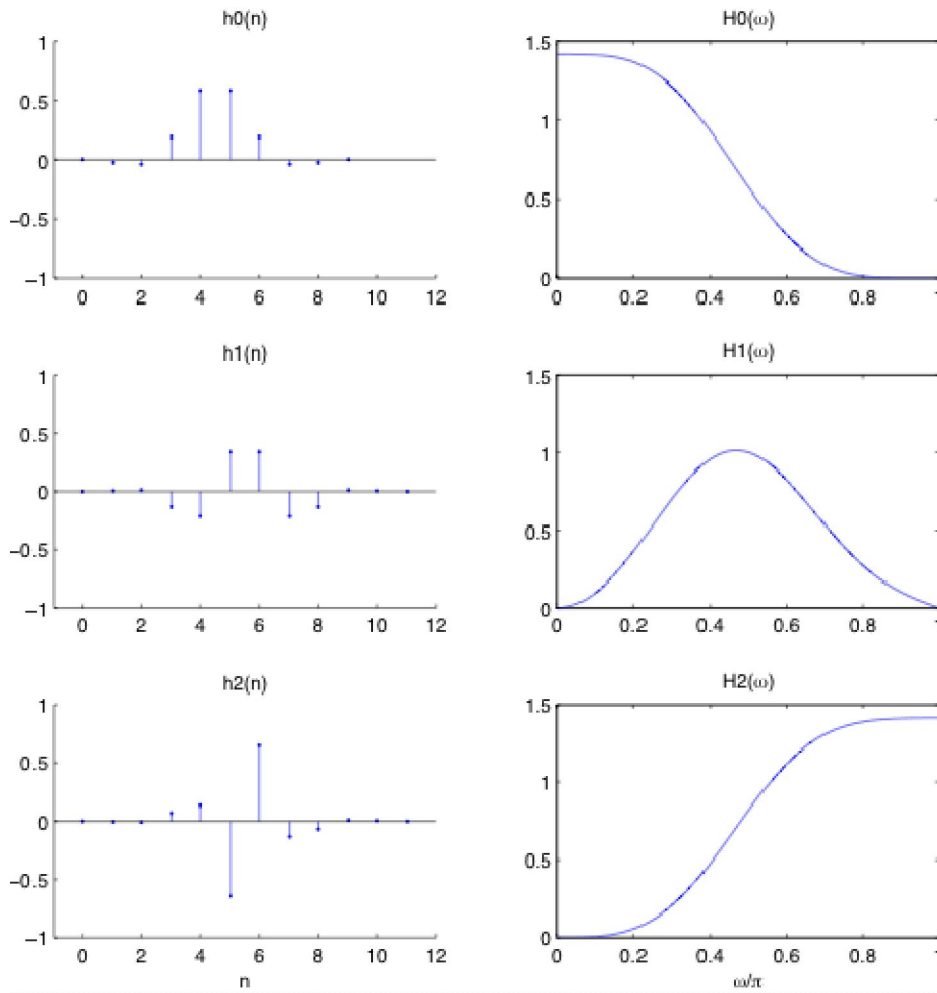


Figure 2: Impulse Responses and Frequency Responses of the Three Filters

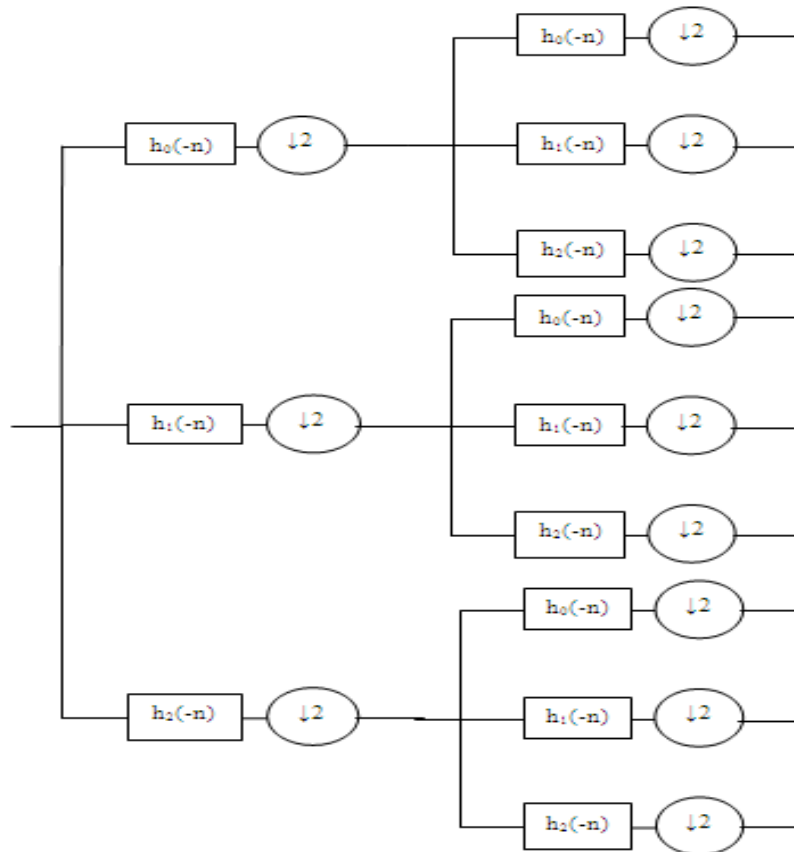


Figure 3. An Oversampled Filterbank for a 2-D Image

3. IHS Color Conversion

The IHS conversion can effectively separate a RGB (Red, Green, Blue) color image into IHS (Intensity, Hue, and Saturation). Intensity (I) refers the total brightness that corresponds to the surface roughness, hue (H) the wavelength contribution and saturation (S) is its purity [8]. The Intensity-Hue-Saturation (IHS) transformation decouples the intensity information from the color carrying information. The hue attribute describes a pure color and saturation gives the degree to which pure color is diluted by white light. This transformation permits the separation of spatial information into one single intensity band. The changes in the

intensity values are not distributed evenly in all the three R, G, and B components when the inverse transform is performed [9]. In fusion, the IHS transformation is used to convert three bands of an MS image from the RGB color space to the IHS color space. The I component is related to the spatial frequencies and is highly correlated with the PAN image. However, PAN has higher spatial frequencies than the MS images. These high frequencies represent the finer details present in the PAN image. Therefore, replacing the I component with the PAN image and transforming back to the RGB color space will introduce high frequencies from PAN into the MS image [10].

4. Proposed Model for SAR Image Fusion

The proposed system for SAR image fusion based framelet transform is shown in Figure (4). The procedure of the proposed system is described as follows:

Step (1): Conversion of multispectral (RGB) image to IHS space image

Step (2): Computation of two dimensions framelet transform.

The two dimensional framelet should be applied to the pan image and I components of SAR image separately.

Step (3): Fusion rule

The fusion rule is key to fusion quality. There are two fusion rules that can be used here for the SAR image fusion. The first rule, the weighted average rule to merge lowpass subband of the two images since they both contain approximations of the sources image. While the second rule, the maximum selection rule just picks the coefficient in each detail subband with the largest magnitude, compare the two coefficients of the two images and select the maximum one, but this rule leads to color distortion. In the paper, the maximum rule is replaced with the following rule

$$\text{Fused image} = K1 * \max(\text{Transform of (image 1), Transform of (image 2)}) + K * \min(\text{Transform of (image 1), Transform of (image 2)}) \quad (10)$$

Where K varies from 0 to 0.5 and $K1=1-K$

Step (4): Inverse fast discrete framelet transforms

After selecting the fused low frequency and high frequency bands, the fused coefficient is reconstructed using the Inverse framelet transform to get the fused image which represents the new I band.

Step (5): Inverse (IHS) to (RGB) image

The resultant image which represents the new I band will be back transformed with the original H & S bands to the RGB model. Then these three bands represent the new MS image.

5. The factors for quantitative analysis

To evaluate fusion results quantitatively, some statistical parameters, such as the combination entropy, the correlation coefficient and the peak signal to noise ratio are employed to describe the contained information in the fused image

- The Combination Entropy

The combination entropy (C.E.) of an image is defined as equation (11) [11]:

$$C.E = -\sum_n p_n \log_2(p_n), \text{bit/pixel} \quad (11)$$

Where: p is the combination probability of the image. The combination entropy represents the amount of information incorporated in fused images.

- Correlation Coefficient:

The closeness between two images can be quantified in terms of the correlation function. The correlation coefficient is computed from [12, 13]

$$\text{corr}(I, F) = \frac{\sum_{r=1}^N \sum_{c=1}^N (I(r,c) - \bar{I})(F(r,c) - \bar{F})}{\sqrt{\left(\sum_{r=1}^N \sum_{c=1}^N (I(r,c) - \bar{I})^2 \right) \left(\sum_{r=1}^N \sum_{c=1}^N (F(r,c) - \bar{F})^2 \right)}} \quad (12)$$

Where I is the original image, F is the fused image, \bar{I} and \bar{F} stand for the mean values of the corresponding data set, and $N \times N$ is the image size. Here I and F are the two images which the correlation is computed between them. The correlation between each band of the multispectral image before and after sharpening was computed. The best spectral information is available in the multispectral image and hence the PAN image bands should have a correlation closer to that between the multispectral image bands. The spectral quality of the sharpened image is good if the correlation values are closer to each other. Another set of correlation coefficients was computed between each band of the multispectral image and the PAN image. Since the PAN image has better spatial

information, the correlation between the sharpened image bands and the pan image is expected to increase compared to that of the original multispectral.

- The Peak Signal to Noise Ratio
The Peak SNR (PSNR) is defined as equation (13) [14]:

$$SNR_{PEAK} = 10 \log \left(\frac{(N-1)^2}{\frac{1}{N} \sum_{r=0}^{N-1} \sum_{c=0}^{N-1} [I(r,c) - \bar{I}(r,c)]^2} \right) \quad (13)$$

Where I is the original image, F is the fused image, and $N \times N$ is the image size. In this measure a larger number implies a better result.

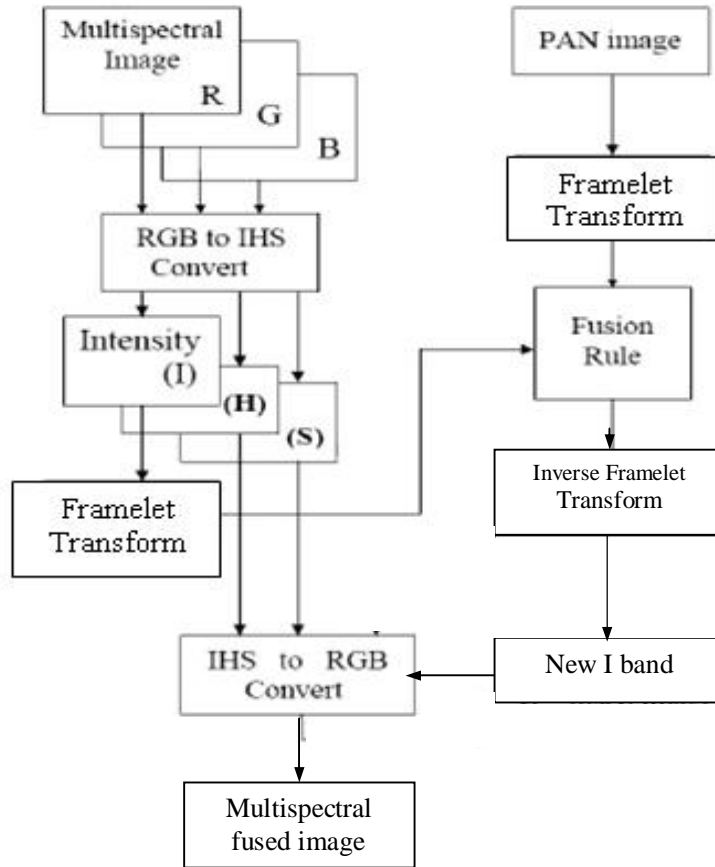


Figure 4: Block Diagram of the Proposed Model

6. Simulation and Result

The SAR Panchromatic and multispectral images are shown in Figures 5(a,b), 6(a,b), 7(a,b) and 8(a,b). The proposed model is applied to this data set to produce the fused multispectral images in figures 5(c), 6(c), 7(c) and 8(c),

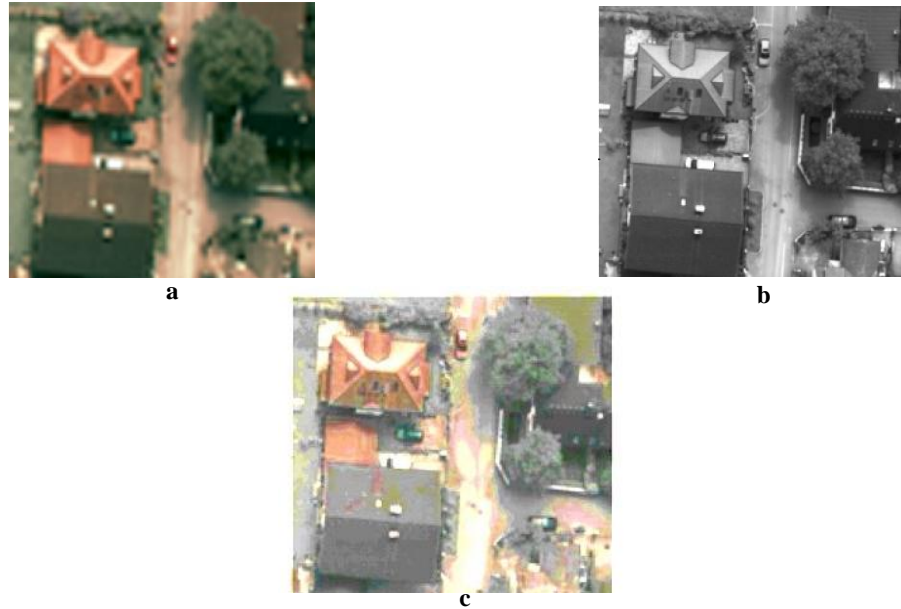


Figure 5. The original SAR images 1 and fused image: (a) the original MS image; (b) the original PAN image; (c) the fused image using our proposed fusion method

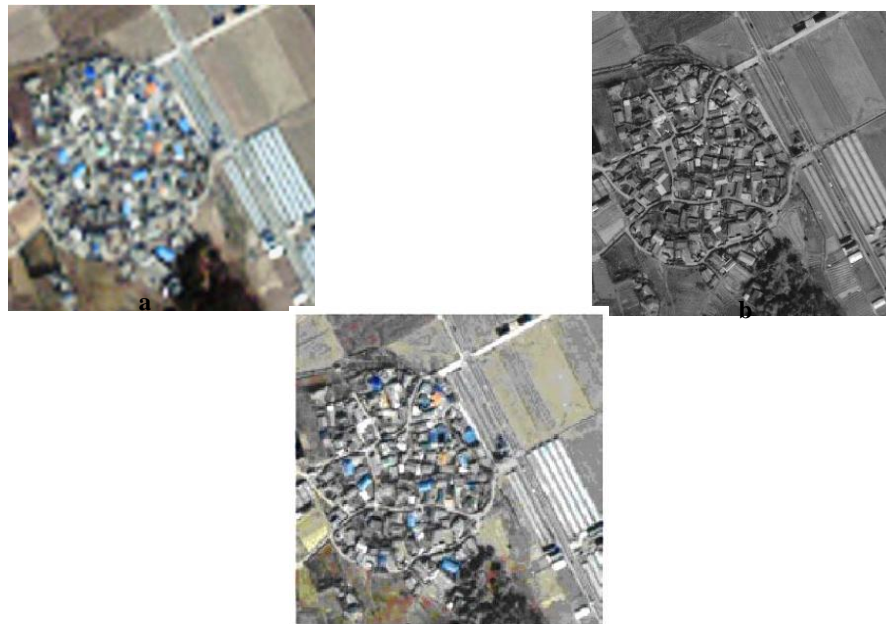


Figure 6. The original SAR images 2 and fused images: (a) the original MS image; (b) the original PAN image; (c) the fused image using our proposed fusion method.

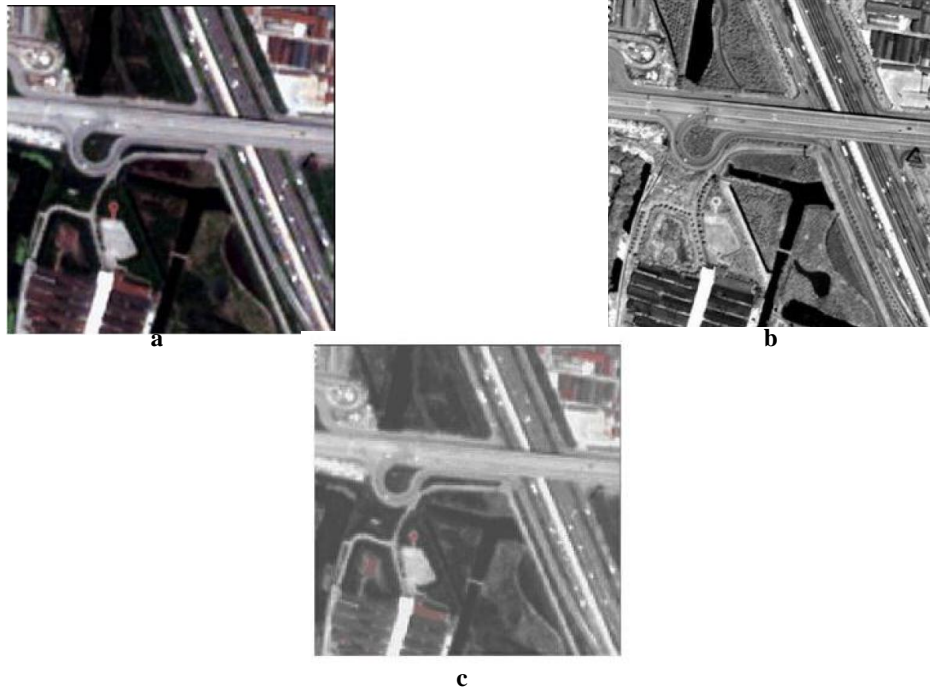


Figure 7. The original SAR images 3 and fused images: (a) the original MS image; (b) the original PAN image; (c) the fused image using our proposed fusion method

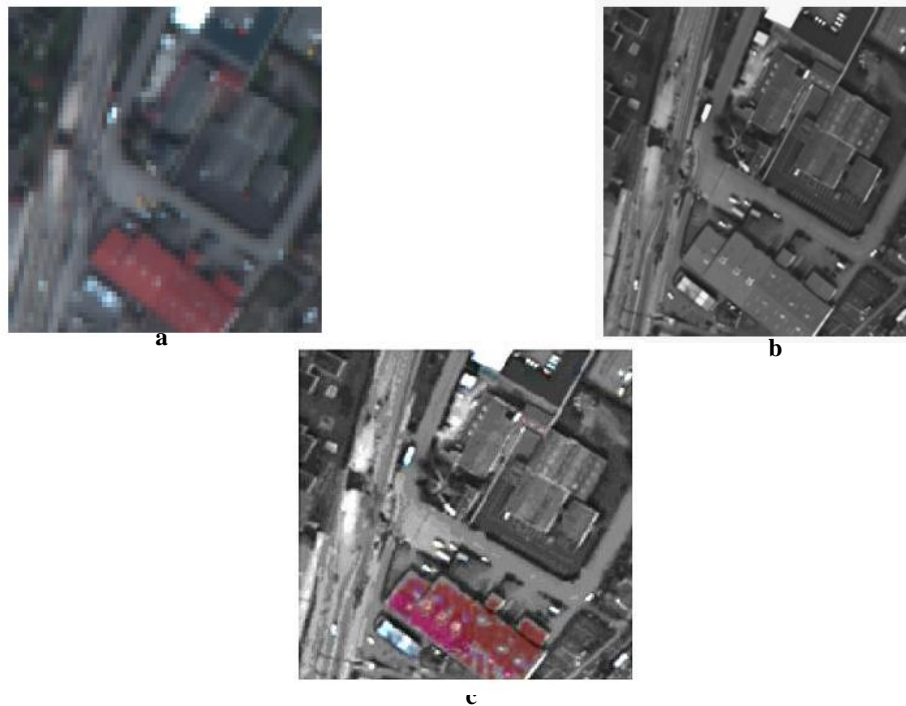


Figure 8. The original SAR images 4 and fused images: (a) the original MS image; (b) the original PAN image; (c) the fused image using our proposed fusion method

a good fusion approach should retain the maximum information from the original images and should not damage the internal relationship among the original bands. From the fused images, they should be noted that both the spatial and the spectral resolutions have been enhanced, in comparison to the original images. The fused image contains both the structural details of the higher spatial resolution panchromatic image and the rich spectral information from the multispectral images. Different fusion methods applied to this data set to produce the fused multispectral images, the combination entropy, correlation coefficient and PSNR were computed as shown in tables (1) and (2). The correlation coefficient and PSNR values are computed between the fused image bands with their corresponding MS image bands, and also computed between the fused image bands with the original panchromatic image. In tables 1 and 2, the combination entropy of the framlet based image fusion is greater than that of the IHS, PCA and DWT methods. The PSNR values between the fused image bands with their corresponding MS image bands (in table 1) indicate that the pixel values are less distorted in the proposed method compared to the IHS, PCA and DWT methods. The correlation coefficient values between each result image band with its original MS band (in table 1) indicate that the proposed fusion method produce the best correlation result. The PSNR values between the fused images bands with the original PAN image (in table 2) indicate that the pixel values are less distorted in the proposed method compared to HIS, PCA and DWT

methods. The correlation coefficient values between each result image band with the original panchromatic image (in table 2) indicate that the proposed fused method produces the closest correlation with the panchromatic bands compared to PCA and DWT methods. Thus, the framlet based image fusion method is superior to the IHS, PCA and DWT methods in terms of combination entropy, PSNR and correlation coefficient and the framlet based image fusion method is very efficient for fusing SAR images.

7. Conclusion

In this paper, method is proposed for fusing SAR images based on the framelet transform and new rules selection. This paper has compared, through analysis and simulation, proposed method, HIS, PCA and wavelet methods for fusing SAR image. Based on the simulation result, it is shown the proposed method provides a good result when it has higher values for the combination entropy, the correlation coefficient and the peak signal to noise ratio for SAR image fused. Also increasing the value of K (from 0 to 0.5) for selection rule in proposed method make the fused image produced better quality.

Table 1

The (Combination Entropy, Correlation Coefficient, PSNR) values between the fused image bands with their corresponding MS image bands computed for the different fusion methods.

| SAR Image | Method | Combination Entropy of fused image | Correlation Coefficient Between each new fused image bands with their corresponding original MS bands | | | PSNR values Between each new fused image bands with their corresponding original MS bands | | |
|-----------|-----------------------|------------------------------------|---|-----------|-----------|---|-----------|-----------|
| | | | R & new R | G & new G | B & new B | R & new R | G & new G | B & new B |
| 1 | IHS | 4.1380 | 0.8539 | 0.8098 | 0.7869 | 65.7045 | 66.8819 | 68.1162 |
| | PCA | 5.0952 | 0.9682 | 0.9537 | 0.9440 | 71.5586 | 72.6991 | 73.9199 |
| | Wavelet | 5.3693 | 0.9680 | 0.9538 | 0.9446 | 71.5323 | 72.7053 | 73.9614 |
| | Framelet with K= 0.1 | 5.4727 | 0.9695 | 0.9554 | 0.9460 | 71.6748 | 72.8400 | 74.0687 |
| | Framelet With K = 0.3 | 5.6584 | 0.9776 | 0.9669 | 0.9596 | 72.8559 | 74.0332 | 75.2676 |
| 2 | IHS | 3.8322 | 0.7678 | 0.7593 | 0.7499 | 63.0350 | 62.9486 | 62.9509 |
| | PCA | 5.0327 | 0.9483 | 0.9466 | 0.9455 | 68.9987 | 68.9122 | 68.9151 |
| | Wavelet | 5.2241 | 0.9409 | 0.9390 | 0.9377 | 68.7866 | 68.7012 | 68.7024 |
| | Framelet with k= 0.1 | 5.3487 | 0.9498 | 0.9482 | 0.9470 | 69.0445 | 68.9579 | 68.9605 |
| | Framelet with k= 0.3 | 5.5741 | 0.9626 | 0.9615 | 0.9607 | 70.1757 | 70.0894 | 70.0917 |

Table 1 (continued)

| SAR Image | Method | Combination Entropy of fused image | Correlation Coefficient Between each new fused image bands with their corresponding original MS bands | | | PSNR values Between each new fused image bands with their corresponding original MS bands | | |
|-----------|----------------------|------------------------------------|---|-----------|-----------|---|-----------|-----------|
| | | | R & new R | G & new G | B & new B | R & new R | G & new G | B & new B |
| 3 | IHS | 4.3220 | 0.7784 | 0.7531 | 0.7428 | 68.5982 | 68.3389 | 67.7877 |
| | PCA | 5.0988 | 0.9325 | 0.9204 | 0.9149 | 74.0433 | 73.7840 | 73.2328 |
| | Wavelet | 5.4276 | 0.9382 | 0.9270 | 0.9217 | 74.4658 | 74.2010 | 73.6438 |
| | Framelet with k= 0.1 | 5.5205 | 0.9403 | 0.9294 | 0.9243 | 74.5827 | 74.3235 | 73.7700 |
| | Framelet with k= 0.3 | 5.6718 | 0.9466 | 0.9368 | 0.9305 | 74.8916 | 74.5694 | 73.9063 |
| 4 | IHS | 4.3706 | 0.6552 | 0.6211 | 0.5934 | 61.0722 | 60.6863 | 60.3297 |
| | PCA | 5.4015 | 0.9272 | 0.9150 | 0.9148 | 66.9713 | 66.5970 | 66.2412 |
| | Wavelet | 5.4607 | 0.8982 | 0.8895 | 0.8861 | 65.9650 | 65.7809 | 65.4116 |
| | Framelet with k= 0.1 | 5.5522 | 0.9297 | 0.9174 | 0.9175 | 67.0637 | 66.6798 | 66.3240 |
| | Framelet with k= 0.3 | 5.6532 | 0.9614 | 0.9542 | 0.9551 | 69.2783 | 68.8923 | 68.5357 |

Table 2
The (Combination Entropy, Correlation Coefficient, PSNR) values between the fused image bands with the original PAN image computed for the different fusion methods

| SAR Image | Method | Combination Entropy of fused image | Correlation Coefficient Between each new fused image bands with the original PAN image | | | PSNR values Between each new fused image bands with the original PAN image | | |
|-----------|----------------------|------------------------------------|--|-------------|-------------|--|-------------|-------------|
| | | | PAN & new R | PAN & new G | PAN & new B | PAN & new R | PAN & new G | PAN & new B |
| 1 | IHS | 4.1380 | 0.9743 | 0.9395 | 0.8411 | 77.4286 | 69.9783 | 65.0104 |
| | PCA | 5.0952 | 0.9322 | 0.9337 | 0.8720 | 69.9618 | 69.9599 | 65.3941 |
| | Wavelet | 5.3693 | 0.9370 | 0.9323 | 0.8660 | 70.3752 | 69.8651 | 65.3112 |
| | Framelet with k= 0.1 | 5.4727 | 0.9425 | 0.9387 | 0.8730 | 70.7405 | 70.1693 | 65.4070 |
| | Framelet with k= 0.3 | 5.6584 | 0.9432 | 0.9401 | 0.8744 | 70.8105 | 70.2266 | 65.4199 |
| 2 | IHS | 3.8322 | 0.9790 | 0.9803 | 0.9735 | 77.6569 | 78.6696 | 76.0071 |
| | PCA | 5.0327 | 0.8918 | 0.8998 | 0.8697 | 68.1559 | 68.3407 | 68.2718 |
| | Wavelet | 5.2241 | 0.8989 | 0.9072 | 0.8787 | 68.8060 | 69.0364 | 68.9048 |
| | Framelet with k= 0.1 | 5.3487 | 0.9054 | 0.9140 | 0.8853 | 69.0110 | 69.2571 | 69.1157 |
| | Framelet with k= 0.3 | 5.5741 | 0.9074 | 0.9161 | 0.8874 | 69.0696 | 69.3192 | 69.1766 |

Table 2 (continued)

| SAR Image | Method | Combination Entropy of fused image | Correlation Coefficient Between each new fused image bands with the original PAN image | | | PSNR values Between each new fused image bands with the original PAN image | | |
|-----------|----------------------|------------------------------------|--|-------------|-------------|--|-------------|-------------|
| | | | PAN & new R | PAN & new G | PAN & new B | PAN & new R | PAN & new G | PAN & new B |
| 3 | IHS | 4.3220 | 0.9758 | 0.9547 | 0.9640 | 74.1657 | 73.4453 | 76.5087 |
| | PCA | 5.0988 | 0.9056 | 0.8944 | 0.9108 | 72.4548 | 72.1576 | 72.9855 |
| | Wavelet | 5.4276 | 0.8654 | 0.8521 | 0.8696 | 71.1788 | 70.9232 | 71.4399 |
| | Framelet with k= 0.1 | 5.5205 | 0.8936 | 0.8819 | 0.8983 | 72.0808 | 71.7902 | 72.4319 |
| | Framelet with k= 0.3 | 5.6718 | 0.8957 | 0.8845 | 0.9012 | 72.1531 | 71.8718 | 72.5397 |
| 4 | IHS | 4.3706 | 0.9189 | 0.9420 | 0.9616 | 68.4169 | 68.8201 | 71.6017 |
| | PCA | 5.4015 | 0.7030 | 0.7493 | 0.7368 | 62.3167 | 62.5541 | 62.8651 |
| | Wavelet | 5.4607 | 0.7547 | 0.8015 | 0.7948 | 63.2924 | 63.6017 | 64.0866 |
| | Framelet with k= 0.1 | 5.5522 | 0.7570 | 0.8038 | 0.7975 | 63.3337 | 63.6439 | 64.1391 |
| | Framelet with k= 0.3 | 5.6532 | 0.7668 | 0.8119 | 0.8062 | 63.3843 | 63.6898 | 64.1980 |

References

- [1] Wei Zhang, Le Yu, 'SAR and Landsat ETM+ image fusion using variational Model' International Conference on Computer and Communication Technologies in Agriculture Engineering, pp.205-207,2010
- [2] Ying Zhang, Yanjun Li, Ke Zhang, Hongmei Wang, Meili Li, 'SAR and Infrared Image Fusion Using Nonsampled Contourlet Transform' International Joint Conference on Artificial Intelligence, pp. 398-401,2009
- [3] Oguz Gungor, Jie Shan, 'Evaluation of satellite image fusion using wavelet transform' <http://www.isprs.org/istanbul2004/comm7/paper/236>
- [4] Wang Min , Peng Dongliang, Yang Shuyuan, 'Fusion of Multi-band SAR Images Based on Nonsampled Contourlet and PCNN', Fourth International Conference on Natural Computation, pp. 529-533
- [5] A. F. Abdelnour and I. W. Selesnick, "Symmetric Nearly Shift-Invariant Tight Frame Wavelets," IEEE Transactions on Signal Processing, vol. 53, no. 1, pp. 231-239,2005
- [6] Myungjin Choi, "Introduction of a Symmetric Tight Wavelet Frame to Image Fusion Methods Based on Substitutive Wavelet Decomposition", <http://amath.kaist.ac.kr/research/paper/06-8.pdf>.
- [7] I. W. Selesnick, "The Double Density DWT", In A. Petrosian and F. G. Meyer, editors, Wavelets in Signal and Image Analysis: From Theory to Practice. Kluwer, 2001.
- [8] Zhang N., Zhong S., 'Adjustable Transforms of ISH and PCA for QuickBird Panchromatic and Multispectral Images'', CISP 08. Congress on Image and Signal Processing, Vol 3, pp. 471-474,2008
- [9] Meenakshisundaram V., 'Quality Assessment of Ikonos and Quickbird Fused Images for Urban Mapping' Department of Geometrics Engineering, University of Galary, 2005
- [10] Zhenhua Li, Leung H., 'Fusion of Multispectral and Panchromatic Images Using a Restoration-Based Method'' IEEE Transaction on Geoscience and Remote Sensing ,Vol. 47, No 5, pp. 1482-1491, May 2009.
- [11] Myungjin Choi, Rae Young Kim, Myeong-Ryong Nam, and Hong Oh Kim, 'Fusion of Multispectral and Panchromatic Satellite Images Using the Curvelet Transform' IEEE Geoscience and remote sensing letters , vol. 2, no. 2pp. 136-140, April 2005
- [12] Dhia Alzubaydi and Walid A. Mahmmoud 'Slantlet Transform for Multispectral Image Fusion' Journal of Computer Science 5 (4): 263-269, 2009
- [13] A. F. Fadhel, 'Multispectral Image Fusion Using Hybrid Transform' A Thesis Submitted to the Department of Electrical Engineering in the University of Baghdad in Partial Fulfillment of the Requirements for the Degree of the Master of Science in Electrical /Control and Computer Engineering, 2007
- [14] Abbas M. 'Data fusion analysis in expansive wavelet domain', Engineering and development journal vol.12, pp. 307-318, 2008